

## Article

# Feasibility of Nickel–Aluminum Complex Hydroxides for Recovering Tungsten Ions from Aqueous Media

Fumihiko Ogata <sup>1</sup>, Saki Kawamoto <sup>1</sup>, Ayako Tabuchi <sup>1</sup>, Megumu Toda <sup>2</sup>, Masashi Otani <sup>2</sup>, Takehiro Nakamura <sup>1</sup> and Naohito Kawasaki <sup>1,3,\*</sup>

<sup>1</sup> Faculty of Pharmacy, Kindai University, 3-4-1 Kowakae, Higashi-Osaka 577-8502, Osaka, Japan; ogata@phar.kindai.ac.jp (F.O.); kawamoto.saki@kindai.ac.jp (S.K.); 2133420006v@kindai.ac.jp (A.T.); nakamura@phar.kindai.ac.jp (T.N.)

<sup>2</sup> Kansai Catalyst Co., Ltd., 1-3-13 Kashiwagi-cho, Sakai-ku, Sakai 590-0837, Osaka, Japan; megumu.toda@kansyoku.co.jp (M.T.); masashi.ootani@kansyoku.co.jp (M.O.)

<sup>3</sup> Antiaging Center, Kindai University, 3-4-1 Kowakae, Higashi-Osaka 577-8502, Osaka, Japan

\* Correspondence: kawasaki@phar.kindai.ac.jp; Tel.: +81-6-4307-4012

**Abstract:** In this study, the adsorption and/or desorption capacity of tungsten ions using nickel–aluminum complex hydroxides was assessed. Nickel–aluminum complex hydroxides at various molar ratios, such as NA11 were prepared, and the adsorption capacity of tungsten ions was evaluated. Precisely, the effect of temperature, contact time, pH, and coexistence on the adsorption of tungsten ions in the water layer was demonstrated. Among the nickel–aluminum complex hydroxides at various molar ratios, the adsorption capacity onto NA11 was the highest of all adsorbents. The sulfate ions in the interlayer of NA11 was exchanged to tungsten ions, that is, the adsorption mechanism was ion exchange under our experimental conditions. Additionally, to elucidate the adsorption mechanism in detail, the elemental distribution and X-ray photoelectron spectroscopy of the NA11 surface were analyzed. Finally, the results indicated that the tungsten ions adsorbed using NA11 could be desorbed (recovered) from NA11 using sodium hydroxide solution. These results serve as useful information regarding the adsorption and recovery of tungsten ions using nickel–aluminum complex hydroxides from aqueous media.

**Keywords:** nickel–aluminum complex hydroxides; tungsten ion; ion exchange; adsorption; recovery



**Citation:** Ogata, F.; Kawamoto, S.; Tabuchi, A.; Toda, M.; Otani, M.; Nakamura, T.; Kawasaki, N. Feasibility of Nickel–Aluminum Complex Hydroxides for Recovering Tungsten Ions from Aqueous Media. *Sustainability* **2022**, *14*, 3219. <https://doi.org/10.3390/su14063219>

Academic Editors: Rajesh Kumar Jyothi, Pankaj Kumar Parhi, Thenepalli Thriveni and Rambabu Kuchi

Received: 25 February 2022

Accepted: 9 March 2022

Published: 9 March 2022

**Publisher's Note:** MDPI stays neutral with regard to jurisdictional claims in published maps and institutional affiliations.



**Copyright:** © 2022 by the authors. Licensee MDPI, Basel, Switzerland. This article is an open access article distributed under the terms and conditions of the Creative Commons Attribution (CC BY) license (<https://creativecommons.org/licenses/by/4.0/>).

## 1. Introduction

To establish a sustainable society, the United Nations Sustainable Development Goals (SDGs) have gained increasing attention worldwide. Precisely, Goals 7 (affordable and clean energy) and 11 (sustainable cities and communities) were adopted for a stable supply of useful materials, such as rare metals. Tungsten (W) is one of the most widely used materials for different applications. Moreover, over 80% of tungsten is produced in China [1,2]. The European Union added “tungsten” to the list of critical raw materials, defined as metals with growing economic importance that might be susceptible to further scarcity [3]. Additionally, tungsten is also one of the most stockpiled rare metals (nickel, manganese, chromium, molybdenum, cobalt, and vanadium) in Japan. However, these useful materials are mostly unrecovered in physicochemical water treatment. Moreover, a report exists regarding the relationship between tungsten ingestion from drinking water and the high rate of leukemia clusters in the western United States of America. However, no evidence exists linking these factors in a previous study [4]. Thus, the development of environmentally friendly and useful water treatment for the removal/desorption of tungsten is necessary for establishing a sustainable society.

Different methods have been evaluated for the removal and/or desorption of tungsten in the water layer. For example, solvent extraction [5], precipitation [6], direct acid leaching [7], biosorption [4], ion exchange [4], and adsorption [8] were reported. Among them, adsorption is one of the most useful methods for removing and/or recovering tungsten ions in the water layer from the point of view simplicity and cost of operation and design. The conventional recycling process of tungsten from water environment and/or tungsten carbide adopted some treatments such as calcination, leaching, adsorption/desorption, crystallization, thermal decomposition, reduction, and carburization [9]. These processes imply relatively high costs, and that they are not environmentally friendly. Therefore, if the adsorption/desorption potential of adsorbent is explored in the recycling process, its value and applicability would be significantly increased. Furthermore, recent works report the application of metal hydroxides prepared from nickel, iron, copper, and cobalt for the oxygen evolution reaction in alkaline media [10–13]. In our previous study, the feasibility of metal complex hydroxides based on iron and magnesium ions to remove tungsten in the water layer was already demonstrated [14]. These results showed the efficient adsorption and desorption of tungsten ions from aqueous solutions. Recently, metal complex hydroxides based on nickel and aluminum ions are useful for adsorption/recovery of oxoanions, such as chromium(VI) ion [15], arsenic(III) ion [16], and phosphate ions [17], in the water layer have been reported. Therefore, it is assumed that nickel–aluminum complex hydroxides can adsorb tungsten ions since tungsten ions usually exist in oxoanions, such as dimeric tungstate ions ( $\text{WO}_4^{2-}$ ) [14]. However, there are no reports on the adsorption/recovery of tungsten ions using nickel–aluminum complex hydroxides.

In this study, the adsorption capacity of tungsten ions using nickel–aluminum complex hydroxides at various molar ratios in the water layer was demonstrated. It also explores the effects of the initial concentration, reaction temperature, reaction time, and pH. Furthermore, the adsorption/recovery mechanism of tungsten ions is investigated herein.

## 2. Materials and Methods

### 2.1. Materials

Nickel(Ni)–aluminum(Al) complex hydroxides at various molar ratios were prepared. The molar ratios of Ni:Al were 3:1 (NA31), 2:1 (NA21), 1:1 (NA11), and 1:2 (NA12), respectively. The synthesis methods and characteristics of these samples have already been previously reported [15,17]. The sample solution was prepared using a standard tungsten solution ( $\text{NaWO}_4$  in  $\text{H}_2\text{O}$ , FUJIFILM Wako Pure Chemical Ind., Ltd., Osaka, Japan). The pH was adjusted using either hydrochloric acid or sodium hydroxide solution (Special grade reagent, FUJIFILM Wako Pure Chemical Ind., Ltd., Osaka, Japan).

### 2.2. Amount of Adsorbed Tungsten Ions

To confirm the adsorption capability of tungsten ions using the NA adsorbents, 0.01 g of each adsorbent and 100 mg/L of tungsten ion solution (50 mL) were reacted, and the sample solutions were shaken (shaking speed: 100 rpm, reaction time: 24 h, temperature: 25 °C). After adsorption, the sample solutions were filtered through a 0.45- $\mu\text{m}$  membrane filter. The concentration of tungsten ions was measured using iCAP-7600 Duo (ICP-OES, Thermo Fisher Scientific Inc., Tokyo, Japan).

### 2.3. Effects of Temperature, Reaction Time, and pH on Adsorption of Tungsten Ions

NA11 of 0.01 g was reacted with 50 mL of tungsten ion solution (from 1 to 100 mg/L). The mixture solution was shaken at 7 °C, 25 °C, or 45 °C for 24 h (shaking speed: 100 rpm). Second, to elucidate the contact time effect, 0.01 g of NA11 was reacted with 50 mL of the sample solution at 100 mg/L. The mixture solution was also shaken for 0.5, 1, 1.2, 3, 6, 9, 16, 20, and 24 h at 25 °C (shaking speed: 100 rpm). Third, to elucidate the effect of the solution pH, 0.01 g of NA11 was mixed with 50 mL of the sample solution at 100 mg/L of pH of 2, 4, 6, 8, 10, and 12. The mixture solution was shaken for 24 h at 25 °C (shaking speed: 100 rpm). After adsorption, the sample solution was separated using a 0.45- $\mu\text{m}$  membrane

filter. The tungsten ion concentration was measured using ICP-OES. Finally, to confirm the adsorption mechanism, the elemental distribution and electron spectroscopy were analyzed using JXA-8530 (JEOL, Tokyo, Japan) and AXIS-NOVA instruments (Shimadzu Co., Ltd., Kyoto, Japan), respectively. The concentration of sulfate ions from NA11 was measured using a DIONEX ICS-900 (Thermo Fisher Scientific Inc., Tokyo, Japan). The experimental conditions have already been described [15].

#### 2.4. Effect of Coexistences on Adsorption of Tungsten Ions

To evaluate the adsorption selectivity of tungsten ions in the water layer, 0.01 g of NA11 was added to the binary solution system (100 mg/L of tungsten ion solution and 100 mg/L of chloride, nitrate, or sulfate ion solution herein). Each anion was prepared using sodium chloride, sodium nitrate, and sodium sulfate. All reagents were purchased from FUJIFILM Wako Pure Chemical Ind., Ltd. (special grade reagent, Osaka, Japan). The mixture solution was shaken for 24 h at 25 °C (shaking speed: 100 rpm). After adsorption, the sample solution was separated using a 0.45- $\mu\text{m}$  membrane filter. The anion concentration was measured by the previously mentioned methods.

#### 2.5. Adsorption and Desorption Capacity of Tungsten Ions Using NA11

To confirm the application of NA11 in water environment fields, the adsorption/desorption capability was evaluated. NA11 of 0.01 g was mixed with 100 mg/L of tungsten ion solution. The amount adsorbed was measured by the previously mentioned method. The collected NA11 after adsorption was reacted with 50 mL of sodium hydroxide or sodium sulfate solutions at various concentration (1, 10, or 100 mmol/L). The reaction mixture was shaken for 24 h at 25 °C (shaking speed: 100 rpm). After desorption, the sample solution was separated using a 0.45- $\mu\text{m}$  membrane filter. The concentration of tungsten ions was measured by the previously mentioned methods.

### 3. Results and Discussion

#### 3.1. Characteristics of NA Adsorbents

As mentioned above, our study previously reported the characteristics of NA adsorbents [17]. Therefore, we briefly described this herein. The SEM images and XRD patterns of the adsorbents are shown in Figure 1. Several peaks, such as (003), (006), (015), and (111), were observed for all samples, indicating that NA samples can be indexed to the stacking of the brucite-like sheets [18]. XRD patterns of NA samples were quite different compared to that of nickel hydroxide. These phenomena suggest that NA samples have been successfully prepared in this study. Additionally, the amorphous structure could be observed with increasing amounts of Al. This result indicates that constituent metals, such as Ni and Al, strongly affect the crystal system. These changes strongly affected the distance between divalent cation and trivalent cation, the distance of interlayer region, and the distance of brucite-like layer in prepared samples. Therefore, the XRD diffraction peaks of nickel hydroxide shifted slightly in this study. In addition, the specific surface areas of NA31, NA21, NA11, and NA12 were 11.7, 15.6, 22.8, and 26.4  $\text{m}^2/\text{g}$ , respectively. Moreover, the amount of hydroxyl groups increased in the order of NA31 (0.82 mmol/g) < NA21 (1.05 mmol/g) < NA12 (1.62 mmol/g) < NA11 (1.92 mmol/g).

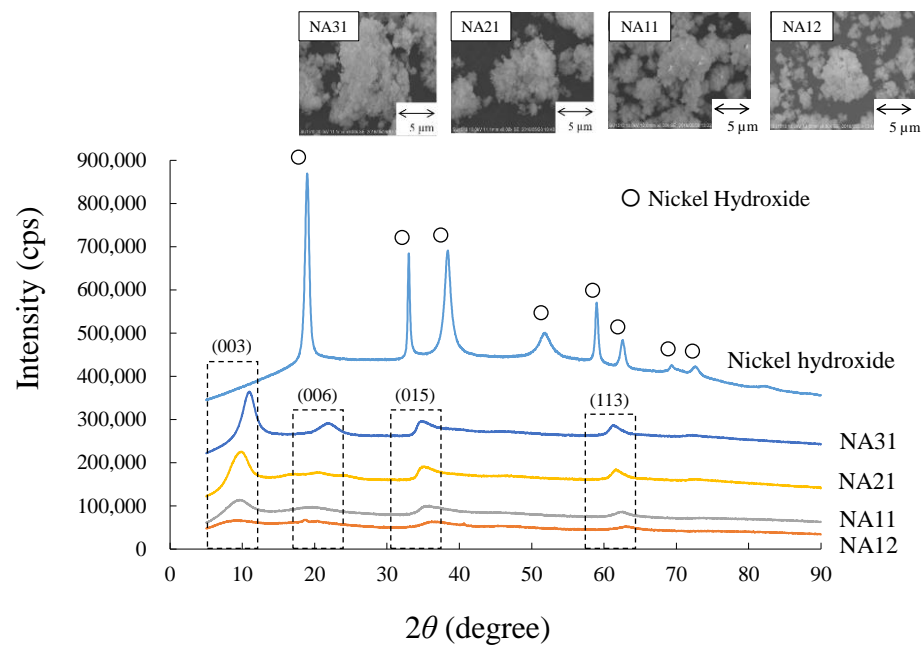


**Figure 1.** Morphological properties and XRD patterns of adsorbents.

### 3.2. Amount of Adsorbed Tungsten Ions Using NA Adsorbents

The amount adsorbed of tungsten ions onto the adsorbents is shown in Figure 2. The tungsten ions adsorbing onto NA11 (~192 mg/g) shows the highest values of all. Similar trends have been previously reported using phosphate ions [17]. Next, we evaluated the relationship between the amount adsorbed of tungsten ions and the physicochemical properties, such as the specific surface area, amount of hydroxyl groups, and surface pH, in detail. Consequently, the correlation coefficient of each parameter was 0.689, 0.855, and 0.913, respectively, for removing tungsten ions in the water layer. Furthermore, Table 1 compares the adsorption of tungsten ions by NA11 with previously reported adsorbents [8,14,16,19]. The amount adsorbed of tungsten ions onto NA11 exceeds that of using other adsorbents. Thus, NA11 is a potential candidate agent for removing tungsten ions in the water layer. Furthermore, NA11 had selectivity for the tungsten ions adsorption.

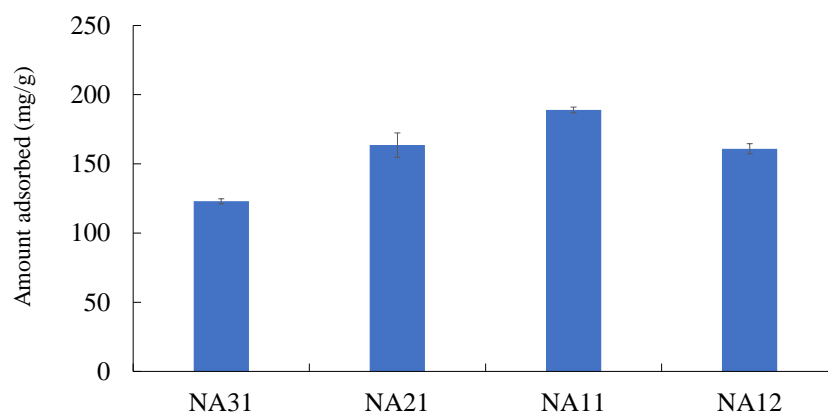


**Figure 2.** Amount adsorbed of tungstate ions by NA11. Concentration: 100 mg/L, amount of adsorbent: 0.01 g, reaction temperature: 25 °C, reaction time: 24 h.

**Table 1.** Comparison of tungstate ions adsorption by NA11 with previously reported adsorbents.

Adsorbents	Adsorption Capability (mg/g)	pH	Temp. (°C)	Initial Concentration (mg/L)	Contact Time (h)	Adsorbent (g/L)	Ref.
Zeolite prepared from fly ash	33.4	2	25	50	24	1	[16]
Al-HT5.0	35.7	6.5–7.0	25	100	24	1	[14]
Fe-HT5.0	48.9	6.5–7.0	25	1000	24	1	[14]
Fe(OH) <sub>3</sub>	53.4	6.7	25	800	22	4	[19]
MnO <sub>3</sub>	37.4	6.7	25	800	22	4	[19]
Fe-Mn binary oxide	65.4	6.7	25	800	22	4	[19]
Chitosan coated clay	11.4–23.9	4–6.4	~25	20–500	24	20	[8]
Natural clay	2.11–5.54	4–6.4	~25	20–500	24	20	[8]
NA11	189.0	-	25	100	24	0.2	This study

### 3.3. Adsorption Isotherms of Tungsten Ions Using NA11

The adsorption isotherms of tungsten ions onto NA11 at different temperatures are shown in Figure 3. The amount adsorbed of tungsten ions increases as the adsorption temperature increases (7 °C < 25 °C < 45 °C). In addition, further study is necessary for elucidating the optimal adsorption temperature of tungsten ions in the water layer. To elucidate the adsorption capability of tungsten ions, the empirical correlations of Langmuir and Freundlich, represented by Equations (1) and (2), have been used to fit the data [20,21].

$$1/q = 1/(q_{max}K_L C_e) + 1/q_{max} \quad (1)$$

$$\log q = \frac{1}{n} \log C_e + \log K_F \quad (2)$$

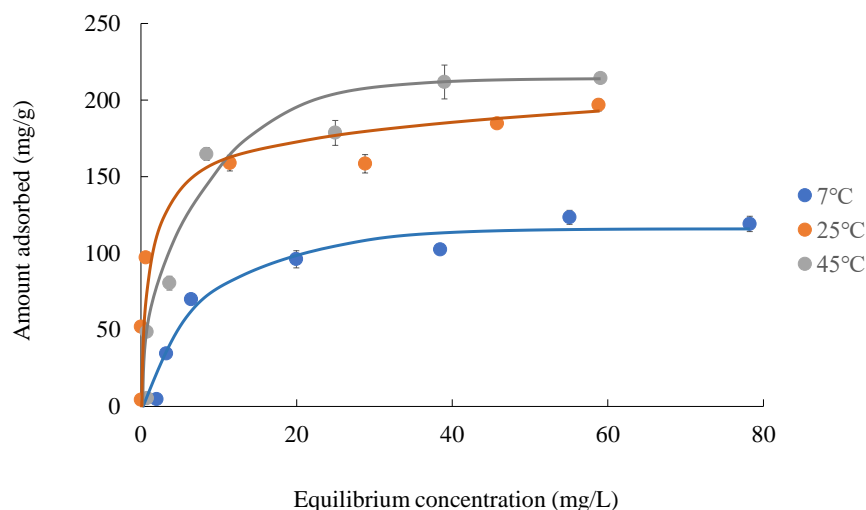


**Figure 3.** Adsorption isotherms of tungstate ions onto NA11. Initial concentration: 1, 10, 20, 40, 60, 80, and 100 mg/L, amount of adsorbent: 0.01 g, reaction temperature: 7, 25, and 45 °C, reaction time: 24 h.

Here,  $q$  is the amount adsorbed of tungsten ions (mg/g),  $q_{max}$  is the maximum amount adsorbed (mg/g), and  $C_e$  is the concentration at equilibrium (mg/L).  $K_F$  and  $1/n$  are the adsorption capacity and adsorption affinity, respectively.  $K_L$  is the Langmuir isotherm constant (binding energy) (L/mg) [4].

The Langmuir and Freundlich models assume that the adsorption site is homogeneous, and all adsorption sites have identical adsorption energy. The adsorption energy decays exponentially as the adsorbent surface coverage increases, respectively. The constants in the Freundlich and Langmuir models for the adsorption of tungsten ions are shown in Table 2. The correlation coefficients for the Freundlich and Langmuir models range from 0.908–0.982

and 0.972–0.979, respectively. Therefore, tungsten ions were probably adsorbed through monomolecular adsorption onto the NA11 surface under our experimental conditions. Additionally, the Langmuir adsorption isotherm is useful for calculating the maximum amount adsorbed ( $q_{max}$ ) of tungsten ions, and  $q_{max}$  increases with the adsorption temperature increasing ( $7\text{ }^{\circ}\text{C}$  (125.0 mg/g) <  $25\text{ }^{\circ}\text{C}$  (175.4 mg/g) <  $45\text{ }^{\circ}\text{C}$  (256.4 mg/g)). These phenomena show similar trends in adsorption isotherms (Figure 3). Finally, tungsten ions were adsorbed onto the NA11 surface when the value of  $1/n$  ranged from 0.1 to 0.5 [22]. However, tungsten ions were difficultly adsorbed onto the NA11 surface when  $1/n > 2$ . Herein, the value of  $1/n$  was 0.15–0.32. Therefore, tungsten ions were facility adsorbed onto the NA11.

**Table 2.** Freundlich and Langmuir constants for the adsorption of tungstate ions.

Adsorbents	Temperatures ( $^{\circ}\text{C}$ )	Langmuir Models			Freundlich Models		
		$q_{max}$ (mg/g)	$K_L$ (L/mg)	$r$	$\log K_F$	$1/n$	$r$
NA11	7	125.0	0.19	0.979	1.7	0.22	0.974
	25	175.4	1.97	0.973	2.0	0.15	0.982
	45	256.4	0.13	0.972	1.8	0.32	0.908

Next, we demonstrated the relationship between the amount of tungsten ions adsorbed and amount of sulfate ions released (Figure 4). Many studies have reported the adsorption (interaction) mechanism, such as electrostatic interaction, ligand exchange, and ion exchange, between the adsorbent and the adsorbate using metal complex hydroxides [14,18,23,24]. Sulfate ions, such as exchange anions, were maintained in the NA11 interlayer herein. Consequently, a positive correlation of 0.988 was confirmed, indicating that ion exchanges between the tungsten and sulfate ions obviously occurred in the sample solution. Moreover, the elemental distribution and X-ray photoelectron spectroscopy were measured before and after adsorption of tungsten ions (Figures 5 and 6). The tungsten and oxygen content increased after the adsorption treatment. Tungsten usually exists as tungstate ions (oxyanions) in the aqueous phase [4]. Therefore, the oxygen intensity increased after adsorption than before adsorption. Finally, we analyzed the binding energy before and after adsorption. After adsorption, W(4d3/2), W(4d5/2), and W(4f5/2) peaks were detected, and these peak intensities significantly increased. Furthermore, the S(2s) and S(2p) peak intensities were decreased after adsorption, suggesting that tungsten ions were adsorbed onto NA11, and simultaneously, sulfate ions in the NA11 interlayer were released. These results support the previously mentioned adsorption mechanism herein.

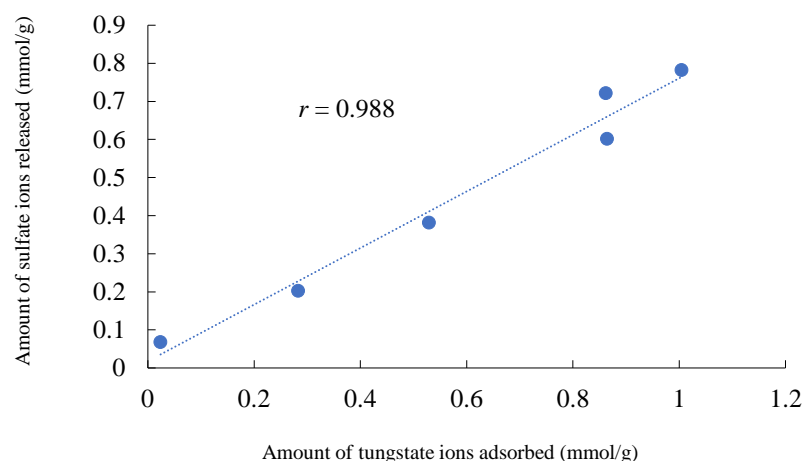


**Figure 4.** Relationship between amount of tungstate ion adsorbed and amount of sulfate ion released. Initial concentration: 1, 10, 20, 40, 60, 80, and 100 mg/L, amount of adsorbent: 0.01 g, reaction temperature:  $25\text{ }^{\circ}\text{C}$ , reaction time: 24 h.

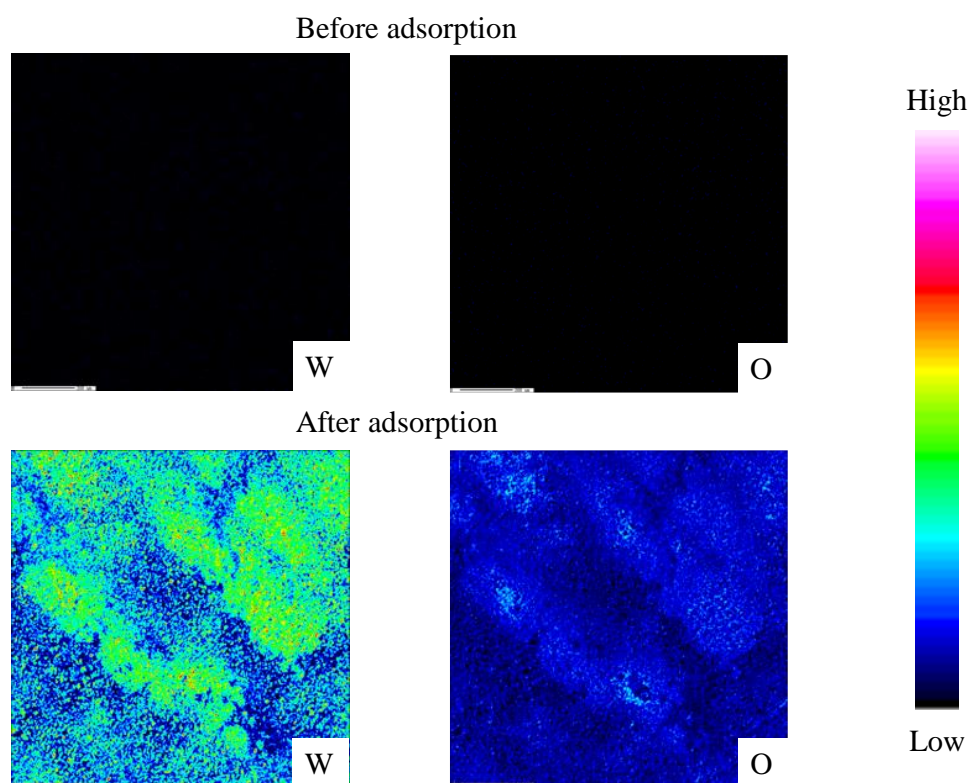


**Figure 5.** Elemental distributions of tungsten (W) and oxygen (O) before and after adsorption using NA11. Concentration: 100 mg/L, amount of adsorbent: 0.01 g, reaction temperature: 25 °C, reaction time: 24 h.

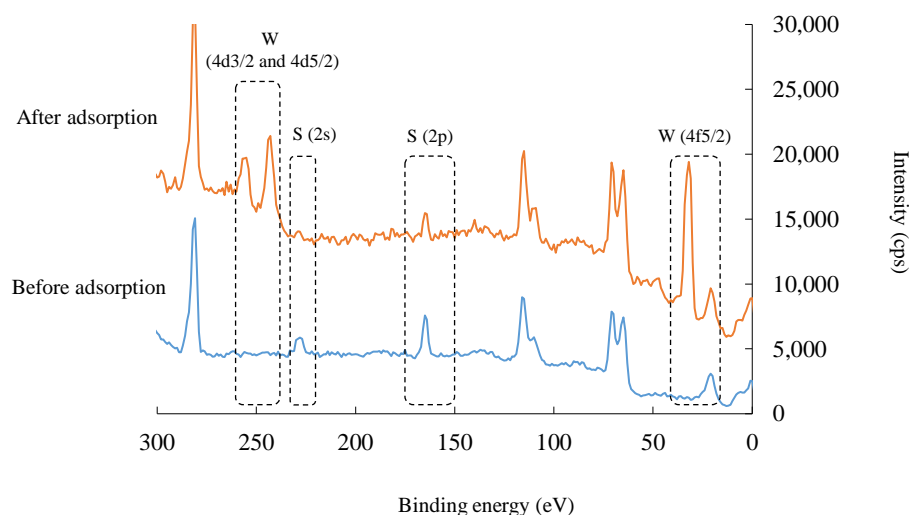


**Figure 6.** X-ray photoelectron spectroscopies of tungsten (W) and oxygen (O) before and after adsorption using NA11. Concentration: 100 mg/L, amount of adsorbent: 0.01 g, reaction temperature: 25 °C, reaction time: 24 h.

### 3.4. Influence of Contact Time on Adsorption of Tungsten Ions Using NA11

The adsorption rate of tungsten ions onto NA11 is shown in Figure 7. The amount adsorbed of tungsten ions increases with the increasing adsorption time. The initial portion of the adsorption process shows the rapid adsorption within an hour because most of the adsorption sites are vacant at the initial portion of the adsorption process. Afterward, the quantity adsorbed increases gradually and alters the equilibrium concentration within 24 h of adsorption. A similar trend was reported in a previous study [4]. Next, the adsorption

kinetics was evaluated since it controls the residence time of the adsorbate adsorption at the solid–liquid interface. Furthermore, these kinetics help develop a pragmatic approach for the design, operation, and optimization of the process. Herein, the pseudo–first-order (PFOM, Equation (3)) [25] and pseudo-second-order (PSOM, Equation (4)) [26] models were selected for representing the adsorption kinetics of tungsten ion in the water layer. These models can be shown as:

$$\ln(q_e - q_t) = \ln q_e - k_1 t \tag{3}$$

$$\frac{t}{q_t} = \frac{t}{q_e} + \frac{1}{k_2 \times q_e^2} \tag{4}$$

where  $q_e$  (mg/g) is the amount adsorbed of tungsten ions at equilibrium,  $q_t$  (mg/g) is the amount adsorbed of tungsten ions at time  $t$ ,  $k_1$  (1/h) is the overall constant in the PFOM, and  $k_2$  (g/mg/h) is the PSOM adsorption constant.

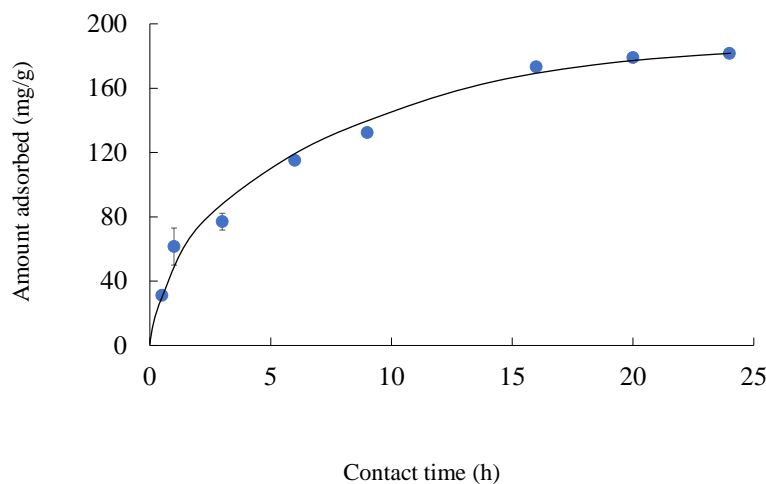


**Figure 7.** Influence of reaction time on the adsorption of tungstate ions onto NA11. Concentration: 100 mg/L, amount of adsorbent: 0.01 g, reaction temperature: 25 °C, reaction time: 0.5, 1, 3, 6, 9, 16, 20, and 24 h.

The calculated parameters were shown in Table 3. From the correlation coefficient ( $r$ ), it is evident that the data were fitted to both the PFOM (0.990) and PSOM (0.994). Additionally, the amount adsorbed of tungsten ions calculated ( $q_e$ ) in the PFOM (191.6 mg/g) and PSOM (208.3 mg/g) models were slightly higher than the actual experimental amount adsorbed of tungsten ions (181.6 mg/g). The obtained results suggest that chemisorption is mainly the interaction mechanism in this study. Previous studies have reported similar trends [27,28].

**Table 3.** Kinetic parameters for the adsorption of tungstate ions using NA11.

Sample	$q_{e,exp}$	PFOM			PSOM		
		$k_1$ (h <sup>-1</sup> )	$q_{e,cal}$ (mg/g)	$r$	$k_2$ (g/mg/h)	$q_{e,cal}$ (mg/g)	$r$
NA11	181.6	4.8	191.6	0.990	$1.3 \times 10^{-3}$	208.3	0.994

### 3.5. Quantity of Tungsten Ions Adsorbed Using NA11 at Different pH Conditions

The pH effect on the removal of tungsten ions onto NA11 was shown in Figure 8. The pH strongly affects the adsorption capacity of tungsten ions onto NA11. The optimal pH condition for the adsorption of tungsten ions was approximately neutral (pH = 6–8) under our experiment. Under acid conditions, tungsten species precipitate to form tungstic acid ( $WO_3 \cdot 2H_2O$ ) and from condensed isopolytungstate ions, such as  $W_{10}O_{32}^{4-}$  [4,13,16].

These phenomena indicate that NA11 showed no excellent adsorption capacity of tungsten ions in the water layer. However, at low pH levels, tungsten ions were attained due to the attractive forces between the tungsten ions (oxyanion) and the positively charged NA11 surface (Surface pH = 7.98) [17,29]. When the pH > 2, the quantity of adsorbed tungsten ions increased and achieved approximately neutral conditions (pH = 6–8). Under neutral conditions, thermodynamically species coexisted, such as the formation of dimetric, trimetric, tetrametric, hexametric species, and the reversible formation of paratungstate A or B, and metatungstate ions in the water layer [4,13]. Finally, under basic conditions, the amount of hydroxide ions increased; thus, the competition between the tungsten (oxide) and hydroxide ions easily occurred in this case. Therefore, the adsorption capacity decreases as the pH increases. Therefore, the tungsten ion adsorption mechanism relates to the complex interaction, such as ion exchange, electrostatic attraction, and surface inner-sphere complex formation [23,24].

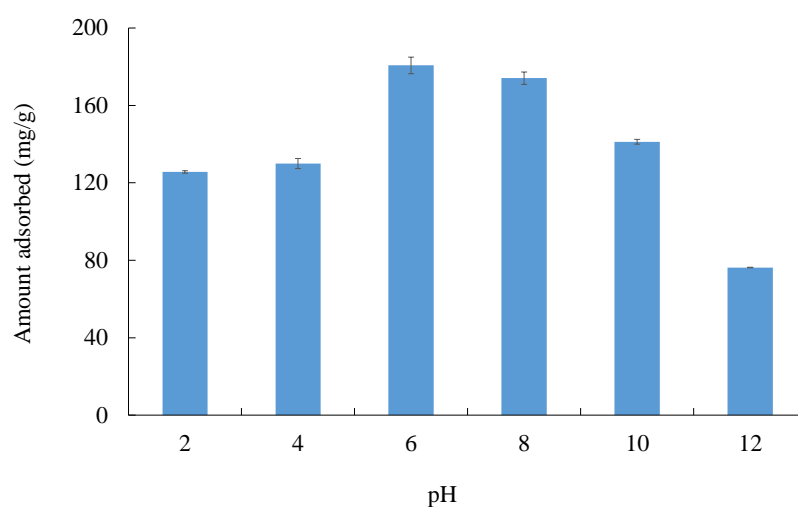


**Figure 8.** Influence of pH on the adsorption of tungstate ions using NA11. Concentration: 100 mg/L, amount of adsorbent: 0.01 g, reaction temperature: 25 °C, reaction time: 24 h.

### 3.6. Adsorption Capacity of Tungsten Ions in a Binary Solution

The adsorption capacity of tungsten ions in a binary solution system is shown in Figure 9. Consequently, chloride and nitrate ions did not strongly influence the adsorption capacity of the tungsten ions. The amount adsorbed of chloride and nitrate ions was 21.3 and 7.8 mg/g, respectively. It can be seen that (1) the interaction between the NA11 and tungsten ions was superior to that of chloride or nitrate ion, and (2) the attraction mechanism between each anion was to form an inner-sphere complex with the hydroxyl groups at the NA11 surface (this observation has already been mentioned in Section 3.2.). Similar phenomena were previously reported [30,31]. Additionally, the amount adsorbed slightly decreased in the binary solution (the case of sulfate and tungsten ions). Furthermore, the sulfate ion concentration increased after adsorption, indicating that the ion exchange between the tungsten and sulfate ions in the NA11 interlayer occurred. Therefore, NA11 is useful for recovering tungsten ions under our experimental conditions.

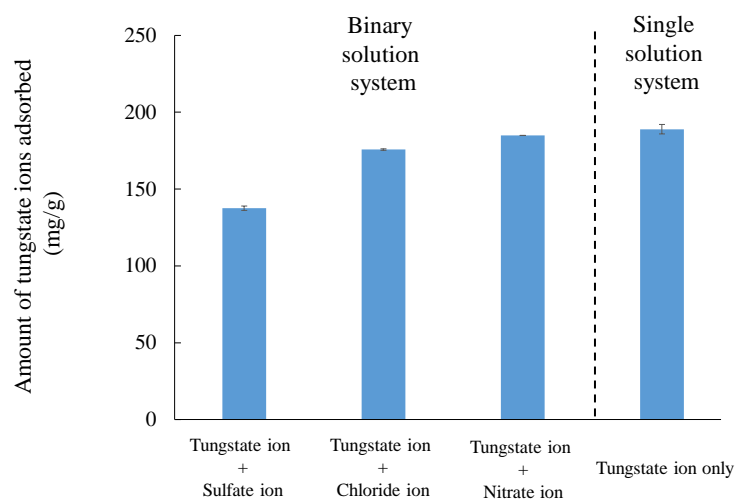


**Figure 9.** Adsorption capability of tungstate ions in binary solution. Concentration: 100 mg/L, amount of adsorbent: 0.01 g, reaction temperature: 25 °C, reaction time: 24 h.

### 3.7. Ad-Desorption Capability of Tungsten Ions by NA11

To elucidate the recovery of tungsten ions from NA11, the adsorption/desorption capacity of tungsten ions using NA11 is shown in Figure 10. Herein, sodium hydroxide and sodium sulfate solutions at various concentrations were used as a recovery solution. The amount desorbed of tungsten ions increases with the increasing concentration of the desorption solution. The recovery percentage of tungsten ions using sodium hydroxide or sodium sulfate solution from 1 to 100 mmol/L was ~40.5%–76.4% or 2.1%–10.5%, respectively. The results obtained suggest that sodium hydroxide solution is more suitable for desorbing tungsten ions than sodium sulfate solution under our experimental conditions. Recently, previous works evaluated hyperspectral image classification and this technique was significantly improved [32,33]. Satellite and/or remote sensing images are useful tools for application of this adsorption/desorption technology using NA11 in the filed works. Therefore, further study is necessary for evaluating the feasibility of NA11 in the field works in the future.

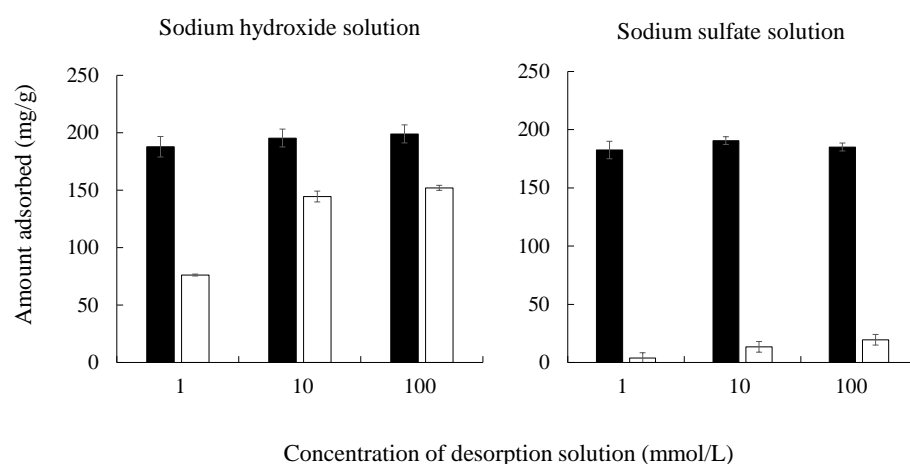


**Figure 10.** Adsorption/Desorption capability of tungstate ions using NA11. Adsorption experimental condition; Concentration: 100 mg/L, amount of adsorbent: 0.01 g, reaction temperature: 25 °C, reaction time: 24 h, desorption experimental condition; Concentration: 1, 10, and 100 mmol/L, reaction temperature: 25 °C, reaction time: 24 h.

#### 4. Conclusions

Our results revealed a high adsorption capacity of tungsten ions using nickel–cobalt complex hydroxide (NA11). The quantity of adsorbed tungsten ions increased as the adsorption temperature and contact time increased. Additionally, the optimal pH condition for removing tungsten ions using NA11 was ~6.0 under our experimental conditions. The factors of the adsorption mechanism of tungsten ions in the water layer were elucidated. Tungsten ions are the ion exchange with the sulfate ions in the NA11 interlayer, and demonstrate physicochemical properties, such as the specific surface area, the amount of hydroxyl groups, and surface pH. Next, NA11 showed a high selectivity adsorption of tungsten ions in a binary solution system, including sulfate, chloride, or nitrate ions. Subsequently, the tungsten ions adsorbed using NA11 could be desorbed from NA11 using sodium hydroxide solution. Therefore, the suggested process for tungsten ion recovery herein allowed a useful recycling treatment. Moreover, NA11 is a promising candidate for the adsorption/desorption of tungsten ions from aqueous media. Finally, further study such as the hyperspectral image classification is necessary for evaluating the feasibility of NA11 in the field works.

**Author Contributions:** Conceptualization, F.O. and N.K.; methodology, M.T. and M.O.; investigation, S.K., A.T. and T.N.; resources, M.T. and M.O.; writing—original draft preparation, F.O. and S.K.; writing—review and editing, F.O. and N.K.; project administration, N.K. All authors have read and agreed to the published version of the manuscript.

**Funding:** This research was supported in part by Kurita Water and Environmental Foundation (21K004) and the Hattori Hokokai Foundation in Japan.

**Institutional Review Board Statement:** Not applicable.

**Informed Consent Statement:** Not applicable.

**Data Availability Statement:** Not applicable.

**Conflicts of Interest:** The authors declare no conflict of interest.

#### References

1. Lende, A.B.; Kulkarni, P.S. Selective recovery of tungsten from printed circuit board recycling unit wastewater by using emulsion liquid membrane process. *J. Water Process Eng.* **2015**, *8*, 75–81. [[CrossRef](#)]
2. Oguchi, T. Materials flow of tungsten. *Met. Resour. Rep.* **2014**, *77*, 296–301.
3. Vollprecht, D.; Plessl, K.; Neuhold, S.; Kittinger, F.; Ofner, W.; Muller, P.; Mischitz, R.; Sedlazeck, K.P. Recovery of molybdenum, chromium, tungsten, copper, silver, and zinc from industrial waste waters using zero-valent iron and tailored beneficiation processes. *Process* **2020**, *8*, 279. [[CrossRef](#)]
4. Gecol, H.; Ergican, E.; Miakatsindila, P. Biosorbent for tungsten species removal from water: Effects of co-occurring inorganic species. *J. Colloid Interface Sci.* **2005**, *292*, 344–353. [[CrossRef](#)] [[PubMed](#)]
5. Paulino, J.F.; Afonso, J.C.; Mantovano, J.L.; Vianna, C.A.; da Cunha, J.W.S.D. Recovery of tungsten by liquid-liquid extraction from a wolframite concentrate after fusion with sodium hydroxide. *Hydrometallurgy* **2021**, *127*, 121–124. [[CrossRef](#)]
6. Cao, C.; Zhao, Z.; Chen, X. Selective precipitation of tungsten from molybdate-containing solution using divalent ions. *Hydrometallurgy* **2011**, *110*, 115–119. [[CrossRef](#)]
7. Mishra, D.; Sinha, S.; Sahu, K.K.; Agrawal, A.; Kumar, R. Recycling of secondary tungsten resources. *Trans. Indian Inst. Met.* **2017**, *70*, 479–485. [[CrossRef](#)]
8. Huo, G.; Peng, C.; Song, Q.; Lu, X. Tungsten removal of from molybdate solutions using ion exchange. *Hydrometallurgy* **2014**, *147*, 217–222. [[CrossRef](#)]
9. Makino, T.; Nagai, S.; Iskandar, F.; Okuyama, K.; Ogi, T. Recovery and recycling of tungsten by alkaline leaching of scrap and charged amino group assisted precipitation. *ACS Sustain. Chem. Eng.* **2018**, *6*, 4246–4252. [[CrossRef](#)]
10. Chen, Y.; Longcheng, Z.; Luchao, Y.; Biao, D.; Yang, C.; Qian, L.; Yonglan, L.; Siyu, L.; Baozhan, Z.; Xuping, S. A NiCo LDH nanosheet array on graphite felt: An efficient 3D electrocatalyst for the oxygen evolution reaction in alkaline media. *Inorg. Chem. Front.* **2021**, *8*, 3162–3166.
11. Bia, D.; Jie, L.; Luchao, Y.; Tingshuai, L.; Qian, L.; Yang, L.; Shuyan, G.; Abdumohsen, A.A.; Khalid, A.A.; Yonglan, L.; et al. CoFe-LDH nanowire arrays on graphite felt: A high performance oxygen evolution electrocatalyst in alkaline media. *Chin. Chem. Lett.* **2022**, *33*, 890–892.

12. Yang, C.; Ting, W.; Xue, L.; Longcheng, Z.; Yonglan, L.; Fang, Z.; Abdullah, M.A.; Jianming, H.; Qian, L.; Xuping, S. A hierarchical CuO@NiCo layered double hydroxide coreshell nanoarray as an efficient electrocatalyst for the oxygen evolution reaction. *Inorg. Chem. Front.* **2021**, *8*, 3049–3054.
13. Peng, D.; Chuqian, M.; Jie, L.; Tingshuai, L.; Yan, W.; Qian, L.; Yonglan, L.; Guanwei, C.; Abdullah, M.A.; Siyu, L.; et al. NiFe layered-double hydroxide nanosheet arrays on graphite felt: A 3D electrocatalyst for highly efficient water oxidation in alkaline media. *Inorg. Chem.* **2021**, *60*, 12703–12708.
14. Ogata, F.; Nakamura, T.; Ueta, E.; Nagahashi, E.; Kobayashi, Y.; Kawasaki, N. Adsorption of tungsten ion with a novel Fe-Mg type hydroxalcite prepared at different  $Mg^{2+}/Fe^{3+}$  ratios. *J. Environ. Chem. Eng.* **2017**, *5*, 3083–3090. [[CrossRef](#)]
15. Ogata, F.; Nagai, N.; Tabuchi, A.; Toda, M.; Otani, M.; Saenjum, C.; Nakamura, T.; Kawasaki, N. Evaluation of adsorption mechanism of chromium(VI) ion using Ni-Al type and Ni-Al-Zr type hydroxides. *Water* **2021**, *13*, 551. [[CrossRef](#)]
16. Ogata, F.; Iwata, Y.; Kawasaki, N. Adsorption of tungsten onto zeolite fly ash produced by hydrothermally treating fly ash in alkaline solution. *Chem. Pharm. Bull.* **2014**, *62*, 892–897. [[CrossRef](#)]
17. Ogata, F.; Toda, M.; Otani, M.; Nakamura, T.; Kawasaki, N. Evaluation of phosphate ion adsorption from aqueous solution by nickel-aluminum complex hydroxides. *Water Sci. Technol.* **2018**, *2017*, 913–921. [[CrossRef](#)]
18. Türk, T.; Alp, İ. Arsenic removal from aqueous solutions with Fe-hydroxalcite supported magnetite nanoparticle. *J. Ind. Eng. Chem.* **2014**, *20*, 732–738. [[CrossRef](#)]
19. Song, Y.F.; He, L.H.; Chen, X.Y.; Zhao, Z.W. Removal of tungsten from molybdate solution by Fe-Mn binary oxide adsorbent. *Trans. Nonferrous Met. Soc. China* **2017**, *27*, 2492–2502. [[CrossRef](#)]
20. Langmuir, I. The adsorption of gases on plane surfaces of glass, mica and platinum. *J. Am. Chem. Soc.* **1918**, *40*, 1361–1403. [[CrossRef](#)]
21. Freundlich, H. Over the adsorption in solution. *J. Phys. Chem.* **1906**, *57*, 384–471.
22. Abe, I.; Hayashi, M.; Kitagawa, M. Studies on the adsorption of surfactants on activated carbon. *J. Jpn. Oil Chem. Soc.* **1976**, *25*, 145–150. [[CrossRef](#)]
23. Li, R.; Wang, J.J.; Zhou, B.; Awasthi, M.K.; Ali, A.; Zhang, Z.; Gaston, L.A.; Lahori, A.H.; Mahar, A. Enhancing phosphate adsorption by Mg/Al layered double hydroxide functionalized biochar with different Mg/Al ratios. *Sci. Total Environ.* **2016**, *559*, 121–129. [[CrossRef](#)] [[PubMed](#)]
24. Yang, K.; Yan, L.G.; Yang, Y.M.; Yu, S.J.; Shan, R.R.; Yu, H.Q.; Zhu, B.C.; Du, B. Adsorptive removal of phosphate by Mg-Al and Zn-Al layered double hydroxides: Kinetics, isotherms and mechanisms. *Sep. Purif. Technol.* **2014**, *124*, 36–42. [[CrossRef](#)]
25. Lagergren, S. Zur theorie der sogenannten adsorption gelöster stoffe, Kunglia Svenska Vetenskapsakademiens. *Handlingar* **1898**, *24*, 1–39.
26. Ho, Y.S.; McKay, G. Pseudo-second order model for sorption process. *Process Biochem.* **1999**, *34*, 451–465. [[CrossRef](#)]
27. Lu, J.; Liu, K.; Zhao, X.; Jefferson, W.; Cheng, F.; Qu, J. Phosphate removal from water using freshly formed Fe-Mn binary oxide: Adsorption behaviors and mechanisms. *Colloid Surf. A Physicochem. Eng. Asp.* **2014**, *455*, 11–18. [[CrossRef](#)]
28. Sposito, G. *The Surface Chemistry of Solids*; Oxford University Press: New York, NY, USA, 1984.
29. Ogi, T.; Makino, T.; Okuyama, K.; Stark, W.J.; Iskandar, F. Selective biosorption and recovery of tungsten from an urban mine and feasibility evaluation. *Ind. Eng. Chem. Res.* **2016**, *55*, 2903–2910. [[CrossRef](#)]
30. Liu, T.; Zheng, S.; Yang, L. Magnetic zirconium-based metal-organic frameworks for selective phosphate adsorption from water. *J. Colloid Interface Sci.* **2019**, *552*, 134–141. [[CrossRef](#)]
31. Wang, J.; Tong, X.; Wang, S. Zirconium-modified activated sludge as a low-cost adsorbent for phosphate removal in aqueous solution. *Water Air Soil Pollut.* **2018**, *229*, 47. [[CrossRef](#)]
32. Hong, D.; Gao, L.; Yao, J.; Zhang, B.; Plaza, A.; Chanussot, J. Graph convolutional networks for hyperspectral image classification. *IEEE Trans. Geosci. Remote Sens.* **2021**, *59*, 5966–5978. [[CrossRef](#)]
33. Hong, D.; Han, Z.; Yao, J.; Gao, L.; Zhang, B.; Plaza, A.; Chanussot, J. SpectralFormer: Rethinking hyperspectral image classification with transformers. *IEEE Trans. Geosci. Remote Sens.* **2022**, *60*, 5518615. [[CrossRef](#)]